Dalton Transactions

ROYAL SOCIETY OF CHEMISTRY

PAPER

View Article Online
View Journal | View Issue

Cite this: *Dalton Trans.*, 2025, **54**, 10627

Facile and efficient synthesis of benzoxazoles and benzimidazoles using a Lewis acid MOF catalyst†

Sarita Kumari, [a] Babita Poonia,[a] Chhaya,[a] Anuzolü,[a] Sarika,[a] Anindita Chakraborty *[a] and Prakash Kanoo *[a,b]

Benzoxazoles and benzimidazoles are a valuable class of heterocyclic compounds and have numerous therapeutic applications. Herein, we present an efficient and facile synthesis of these compounds using a 3D metal–organic framework (MOF), $\{Mn_2(TPA)_2(DMF)_2\}_n$, referred to as the **Mn-TPA** MOF ($TPAH_2$ represents terephthalic acid and DMF denotes *N*,*N*-dimethylformamide) as a catalyst. The desolvated MOF, **Mn-TPA^{Desolv}**, with its robust nature and manganese open metal sites (OMSs) serves as an effective heterogeneous catalyst. **Mn-TPA^{Desolv}** efficiently facilitates the synthesis of benzoxazole and benzimidazole derivatives *via* the reaction of *o*-aminophenol or *o*-phenylenediamine with various aromatic aldehydes. We recorded high conversions up to 99.9% in both the reactions under optimised conditions within a short reaction time. The catalytic reactions exhibited a remarkably high turnover number (TON) up to 9990, and a turnover frequency (TOF) up to 333 min^{-1} for various substrates. Notably, **Mn-TPA^{Desolv}** showed excellent catalytic activity for sterically hindered substrates, such as 1-naphthaldehyde and 9-anthracenecarboxaldehyde, maintaining high TON and TOF values. Furthermore, the recyclability of **Mn-TPA^{Desolv}** revealed that the catalyst could be reused up to 30 cycles with no loss in its structural integrity and catalytic performance. The results obtained in this study demonstrate the excellent catalytic performance of **Mn-TPA^{Desolv}** and emphasize its potential as a scalable, robust, cost-effective catalyst with its broad substrate scope compatibility.

Received 28th February 2025,
Accepted 8th June 2025

DOI: 10.1039/d5dt00500k

rsc.li/dalton

Introduction

Benzoxazoles and benzimidazoles are an important class of heterocyclic compounds.[1] They are distinctive motifs found in the structures of various biological compounds and natural products.[2] The derivatives of both benzoxazoles and benzimidazoles have numerous therapeutic applications, including antifungal, antimicrobial, antitumor, anti-inflammatory, antiprotozoal, antiulcer and antiviral agents targeting various viruses such as HIV and influenza.[1,3–6] The synthesis of novel benzimidazole and its derivatives is a primary focus in medicinal research.[6] Various methods for the synthesis of benzoxazole and benzimidazole derivatives from different reactants have been described in the literature, such as the reaction between *o*-phenylenediamine/*o*-aminophenol with aldehydes and carboxylic acids.[7] For these reactions, different homogeneous and heterogeneous catalytic systems have been reported such as $VOSO_4$, DBU, Pt–TiO_2, $Pd(OAc)_4$, $Yb(OTf)_3$, Fe_3O_4–SiO_2–$(NH_4)_6Mo_7O_{24}$, $CuFe_2O_3$-nanoparticles, graphene oxide, Cu–I nanoparticles, copper-triflate, metal triflates like $Sc(OTf)_3$, H_3O_2/HCl, and lanthanides serving as Lewis acid catalysts.[8–17] Some other catalysts catalyse this oxidative condensation with aldehydes like oxygen,[18] nitrobenzene,[19] 1,4-benzoquinone,[20] DDQ,[21] MnO_2,[22] Zn-proline,[23] H_2O_2/CAN,[24] $Na_2S_2O_5$,[25] $FeCl_3{\cdot}6H_2O$,[26] and Pd–C.[27] Many of these methods suffer from various drawbacks such as low conversion, high temperature, excessive loading of catalysts, extended reaction time, severe reaction conditions, expensive catalysts, low recyclability of catalysts, byproduct formation, and challenges in product isolation and catalyst recovery.[28–30] Consequently, developing a simple and more effective catalytic system for synthesizing benzoxazole and benzimidazole derivatives is essential. Recently, metal–organic frameworks (MOFs) have gained significant attention as heterogeneous catalysts for various organic transformation reactions.[31–33]

MOFs are a class of porous organic–inorganic hybrid materials.[34] They exhibit unique properties, such as high surface area, high porosity, high flexibility, crystalline nature and good thermal stability.[34–37] These unique characteristics

[a]*Department of Chemistry, School of Basic Sciences, Central University of Haryana, Jant-Pali, Mahendergarh 123031, Haryana, India. E-mail: prakashkanoo@jnu.ac.in, achakraborty@cuh.ac.in*

[b]*Special Centre for Nano Sciences, Jawaharlal Nehru University, New Mehrauli Road, New Delhi, Delhi 110067, India*

†Electronic supplementary information (ESI) available: FTIR spectra, PXRD, TGA, NH_3-TPD, SEM, ^1H NMR spectra and tables. See DOI: https://doi.org/10.1039/d5dt00500k

make MOFs ideal for various applications, including drug delivery,[38,39] gas adsorption,[40] gas separation,[41] bio-sensing[42] and catalysis including photocatalysis,[43–49] optical sensing,[50] energy storage,[51,52] *etc*. The use of MOFs as heterogeneous catalysts for organic transformations offers a promising way for sustainable chemistry while minimizing the use of harmful chemicals. These materials combine the advantages of clean synthesis and heterogeneous catalysis, resulting in a simpler workup process, which is particularly attractive from an industrial perspective.[7] MOFs as heterogeneous catalysts play a crucial role in various organic transformations such as the cyanosilylation reaction,[53,54] Knoevenagel condensation,[55] aldol condensation,[56] Michael addition,[57] Henry reaction,[58] cycloaddition of CO_2 to epoxides,[53,59] one-pot cascade reaction,[60] *etc*. MOFs involve direct methods using *o*-phenylenediamine/*o*-aminophenol and aldehydes for condensation to produce benzimidazoles/benzoxazoles, offering a more efficient approach compared to older methods. To address the limitations of traditional methods, MOFs have emerged as promising alternative catalytic systems due to their high surface area, tunable structure and efficient catalytic properties. These properties allow for faster reactions with higher yields and better diffusion of reactants and products. MOFs also improve selectivity and efficiency, provide high recyclability, and are easily separable from the reaction mixture, unlike traditional homogeneous catalysts. Several studies have highlighted the use of MOFs as catalytic systems for the synthesis of benzoxazole and benzimidazole derivatives.[3,4,7,61–63]

Recently, Gong and co-workers developed a catalytic system, MOF@MT-COF–Cu, to synthesize benzimidazole and benzothiazole derivatives under green and mild conditions.[61] Recently, Kim *et al*. reported the oxidative coupling of 2-aminophenols and aldehydes to benzoxazoles using TEMPO-immobilized MOFs.[62] Similarly, Sivakumar *et al*. studied the catalytic activity of MOFs for the synthesis of benzimidazole and benzothiazole derivatives.[4] The catalytic activity of MIL-101(Cr) for the clean synthesis of benzoxazoles has been reported by Khalafi-Nezhad and co-workers.[7] A superacid hafnium-based MOF as a catalyst has been developed by Tran *et al*. for the synthesis of benzoxazoles.[63] Additionally, Maji and co-workers studied the synthesis of benzimidazole derivatives using anionic MOFs as heterogeneous catalysts.[3]

Many of these reported MOF catalytic systems used in the synthesis require high temperatures, reactions take longer time and the conversions are comparatively low. To overcome these drawbacks, herein we demonstrate the use of a simple 3D MOF for the synthesis of benzoxazole and benzimidazole derivatives which takes a short time for the reaction completion at 30 °C and the conversion is up to 99.9%. The MOF, $\{Mn_2(TPA)_2(DMF)_2\}_n$, denoted as **Mn-TPA**, has been synthesized *via* the solvothermal method in high yield ($TPAH_2$ is terephthalic acid and DMF stands for *N*,*N*-dimethylformamide).[53,54,64] The starting materials for preparing the **Mn-TPA** MOF are readily accessible and cost-effective, making it an affordable catalyst. The synergistic effect of manganese and terephthalic acid (H_2TPA) is crucial both in the formation of the structure of **Mn-TPA** and the functional properties of the MOF. The manganese ions from $Mn(NO_3)_2{\cdot}4H_2O$ act as coordination centers, linking the TPA ligands through terephthalate groups, thus forming a stable **Mn-TPA** network. It is interesting to note that the coordination number of manganese is six in **Mn-TPA** while it reduces to four in **Mn-TPA^{Desolv}**.[53] This coordination number change is facilitated by a structural rearrangement which involves the breaking of some Mn–O bonds involving manganese and the terephthalate ligand. This synergy between the metal and ligand enhances the framework's structural integrity, making it suitable for applications in catalysis. The activation of the **Mn-TPA** MOF generates manganese open metal sites (OMSs), which behave as Lewis acid sites and result in the formation of **Mn-TPA^{Desolv}**. Due to the presence of abundant OMSs, **Mn-TPA^{Desolv}** effectively functions as a heterogeneous catalyst for the synthesis of benzoxazole and benzimidazole derivatives through the reaction of *o*-aminophenol or *o*-phenylenediamine with various aromatic aldehydes (Scheme 1). The reactions were carried out in ethanol at 30 °C with both electron-withdrawing and electron-donating groups present on aldehyde substrates. A minimal amount of catalyst (0.005–0.006 mmol) was used providing a high TON up to 9990 and a TOF up to 333. 99.9% conversions were achieved for eight aromatic aldehydes in benzoxazoles and thirteen aromatic aldehydes in benzimidazoles within 30–90 min. The catalyst demonstrated remarkable recyclability in the benzimidazole reaction, maintaining 99.9% conversion across 30 cycles. Notably, bulkier aldehydes such as 1-naphthaldehyde and 9-anthracenecarboxaldehyde also reached 99.9% conversion in a short time. We propose that the pores of **Mn-TPA^{Desolv}** facilitate the diffusion of smaller aldehydes, enabling efficient interaction with Lewis acid manganese open metal sites (OMSs) for complete conversion, while larger aldehydes interact with manganese OMSs on the catalyst surface, ensuring full conversion.

Results and discussion

Characterization of Mn-TPA and Mn-TPA^{Desolv}

For catalytic experiments, bulk quantity of **Mn-TPA** was prepared following the procedure outlined in ref. 53, 54 and 64. Both **Mn-TPA** and **Mn-TPA^{Desolv}** were characterized using various techniques including FT-IR, PXRD, TGA, and NH_3-TPD profiles (Fig. S1–S6†). FTIR analysis of **Mn-TPA** and **Mn-TPA^{Desolv}** revealed the peaks of expected functional groups from its starting materials (Fig. S1 and S2†). The phase purity of the as-synthesized samples of **Mn-TPA** and activated **Mn-TPA^{Desolv}** was analysed by comparing its PXRD pattern with the simulated pattern calculated from single-crystal data (Fig. S3†). The activated MOF shows extra peaks in the PXRD pattern, which suggest structural transformation upon removal of coordinated DMF molecules. TGA analysis of **Mn-TPA** provided insights into its weight loss and thermal stability (Fig. S4†). TGA of **Mn-TPA^{Desolv}** confirmed that the activated MOF undergoes significant weight loss only above 400 °C, indicating com-

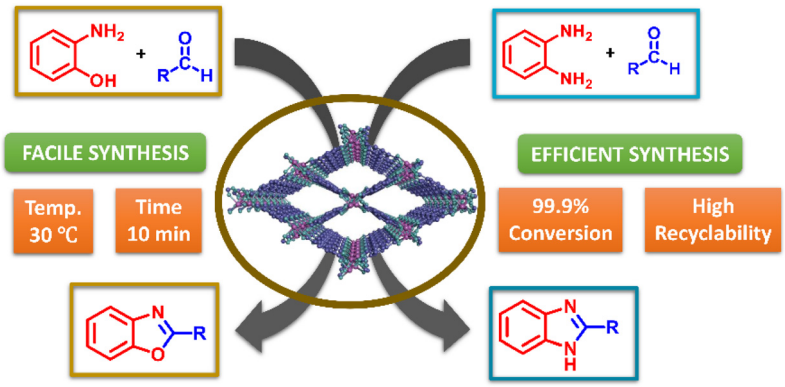

Scheme 1 **Mn-TPA^{Desolv}** MOF as a promising heterogeneous catalyst for the synthesis of benzoxazole and benzimidazole derivatives.

plete removal of DMF molecules from **Mn-TPA^{Desolv}** during the activation process (Fig. S5†). The Lewis acidity of **Mn-TPA^{Desolv}** was investigated using NH_3-TPD experiments, which showed that weak and medium-to-strong acidic sites are present in **Mn-TPA^{Desolv}** (Fig. 1 and S6†). The morphologies of **Mn-TPA** and **Mn-TPA^{Desolv}** were studied using SEM (Fig. S7 and S8†). The SEM images of **Mn-TPA** reveal block shaped crystals with some crystals having a rhombohedral morphology. The images of **Mn-TPA^{Desolv}** reveal smaller blocks compared to **Mn-TPA**.

X-ray photoelectron spectroscopy (XPS) analysis

XPS was employed to analyze the chemical composition and oxidation state of elements present in **Mn-TPA^{Desolv}**. The wide-scan spectrum (Fig. 2a) reveals the presence of manganese (Mn), oxygen (O), and carbon (C), confirming the successful incorporation of these elements into the framework. The high-resolution C 1s spectrum (Fig. 2b) exhibits two prominent peaks with binding energies of 284.3 eV and 288.2 eV, corresponding to the C–C and C═O bonds, respectively, which are characteristic of aromatic and carboxylate functionalities.[65] Similarly, Fig. 2c shows the detailed O 1s spectrum of **Mn-TPA^{Desolv}**, with peaks at 531.4 eV, which is attributed to oxygen in O–C═O environments, indicating the coordination of carboxylate groups to the metal centres. The high-resolution Mn 2p spectrum (Fig. 2d) shows two main peaks due to Mn $2p_{3/2}$ and Mn $2p_{1/2}$. When the Mn $2p_{3/2}$ peak was deconvoluted, we observed two peaks at 641.1 eV and 642.8 eV. These two peaks are attributed to the presence of Mn(II) and Mn(III) in the activated MOF.[66] The presence of variable oxidation states of manganese in **Mn-TPA^{Desolv}** is advantageous for carrying out Lewis acid catalytic reactions.

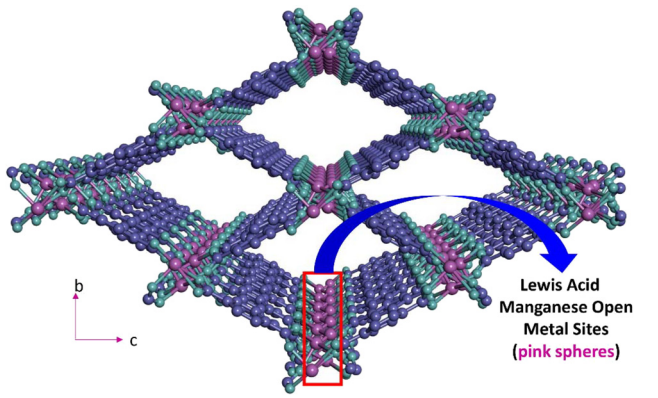

Fig. 1 3D view of **Mn-TPA^{Desolv}** clearly shows the presence of Lewis acidic manganese sites in the channels. Color codes: manganese, pink; carbon, light blue; and oxygen, cyan.

Catalytic study

In order to achieve facile conversion, it is important that the substrate molecules interact efficiently with the **TPA-MOF^{Desolv}** catalyst. Majority of the substrate molecules are polar in nature and contain functional groups such as –CHO, –OH, $–NH_2$, *etc*. The substrates *o*-phenylenediamine/*o*-amino phenol contain amino/hydroxyl groups and are capable of forming hydrogen bonds with the terephthalate groups of the TPA ligand through carboxylate groups. Furthermore, the aromatic rings of *o*-phenylenediamine and *o*-amino phenol may involve in π–π stacking interactions with the aromatic benzene rings of the TPA ligand, providing additional stability to the structure of substrate–framework intermediate. These non-covalent interactions influence the framework properties, such as the porosity, flexibility, and overall performance of the **Mn-TPA^{Desolv}** MOF in catalysis.

Synthesis of benzoxazole derivatives

The permanent porosity and presence of abundant open metal sites within the activated **Mn-TPA^{Desolv}** MOF prompted us to investigate its potential as a Lewis acid catalyst for the synthesis of benzoxazole derivatives. Initially several reactions were performed to optimize the catalyst loading, reaction temperature and time to obtain high conversion. **Mn-TPA** was activated at 120 °C for 12 h under high vacuum before conducting catalytic reactions. For optimization, *o*-aminophenol (1 mmol) and *p*-tolualdehyde (1.1 mmol) were selected as model substrates to carry out reactions in ethanol. When

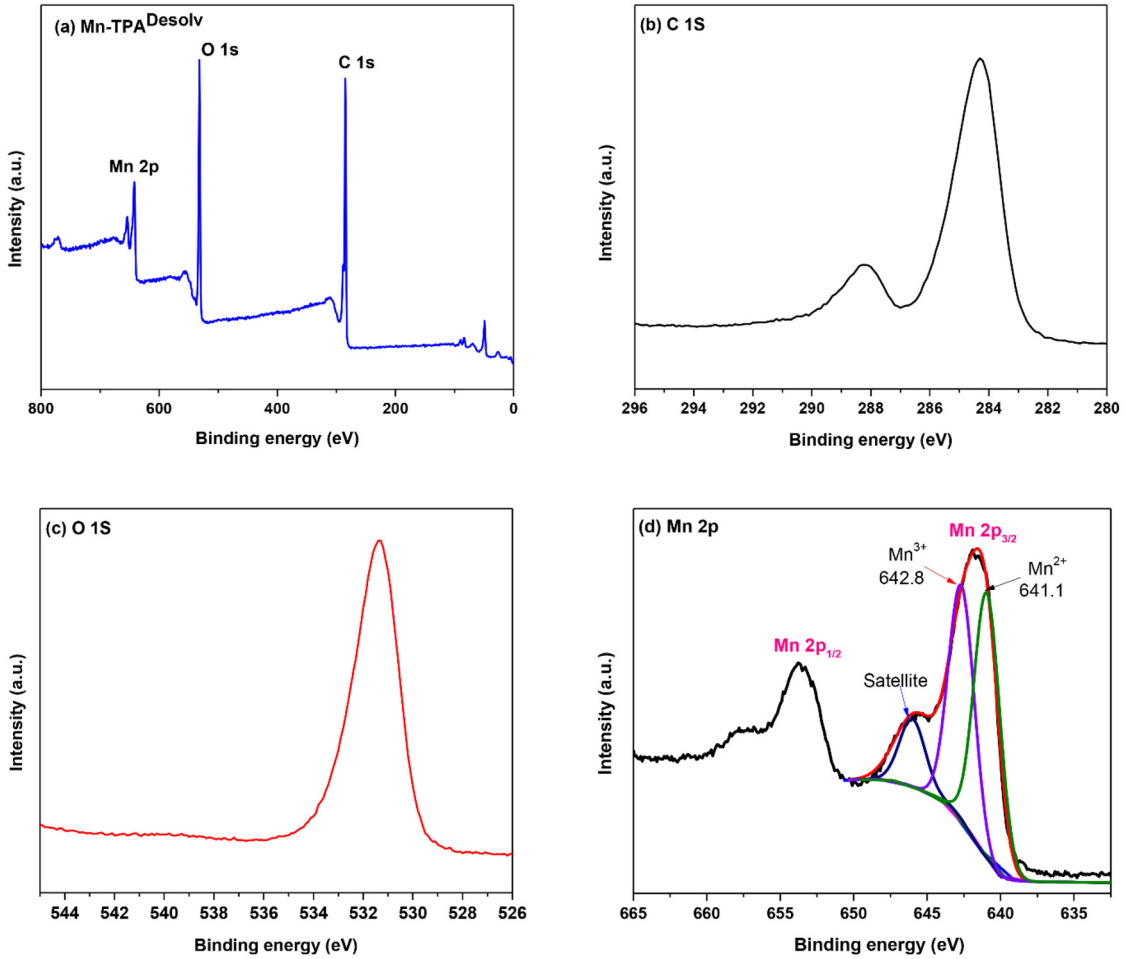

Fig. 2 XPS spectra of **Mn-TPA**^{Desolv}: (a) complete survey scan of **Mn-TPA**^{Desolv}; (b) C 1s spectrum of **Mn-TPA**^{Desolv}; (c) O 1s spectrum of **Mn-TPA**^{Desolv}; and (d) Mn 2p spectrum of **Mn-TPA**^{Desolv}.

1 mmol aldehyde was used with 1 mmol aminophenol, the *o*-aminophenol was not completely consumed. Therefore, 1.1 mmol aldehyde was used to achieve maximum conversion in the reaction. When 0.005 mmol **Mn-TPA**^{Desolv} was used at 30 °C, the conversion reached 79% within 10 min (entry 1, Table S1†). Further the reactions were carried out using 0.006 mmol catalyst in 6 and 8 min, which led to 70% and 81% conversions, respectively (entries 2 and 3, Table S1†). However, using 0.006 mmol of **Mn-TPA**^{Desolv} catalyst at 30 °C for 10 min resulted in an impressive 99.9% conversion (entry 4, Table S1†). To prioritize low energy consumption, a temperature of 30 °C and a reaction time of 10 min were selected as the best optimised conditions. On increasing the catalyst loading to 0.007–0.008 mmol under similar reaction conditions led to 99.9% conversion of benzoxazole derivatives without any change in the reaction time (entries 5 and 6, Table S1†). Upon increasing the reaction temperature to 40 °C and 50 °C using 0.006 mmol **Mn-TPA**^{Desolv}, a 99.9% conversion was achieved in 8 min (entries 7 and 8, Table S1†). The as-synthesized MOF, **Mn-TPA**, achieved a conversion of 55%, which is significantly lower than that of the desolvated MOF (entry 9, Table S1†). It emphasizes the critical role and efficiency of OMSs in enhancing conversion rates. The acid ligand (TPA) did not facilitate any conversion, while the metal source Mn $(NO_3)_2{\cdot}4H_2O$ exhibited only 16% conversion under the optimized conditions (entries 10 and 11, Table S1†). The reaction did not proceed at all in the absence of a catalyst (entry 12, Table S1†). The results demonstrate the necessity of using **Mn-TPA**^{Desolv} as a catalyst rather than the as-synthesized MOF or its individual components. It is worth noting that 0.006 mmol **Mn-TPA**^{Desolv} provided adequate active acidic sites, enabling the reaction to proceed effectively with excellent conversion. Consequently, a catalyst loading of 0.006 mmol **Mn-TPA**^{Desolv} was selected for subsequent catalytic reactions.

Effect of solvents towards the synthesis of benzoxazole derivatives

Solvents play a crucial role in catalytic reactions, and their influence varies depending on the specific catalyst used. Therefore, for this reaction, we have tested various solvents such as water, dichloromethane, chloroform, acetonitrile, hexane, tetrahydrofuran and ethanol. This reaction proceeds

Table 1 Synthesis of benzoxazole derivatives using *p*-tolualdehyde and **Mn-TPA^{Desolv}** in different solvents

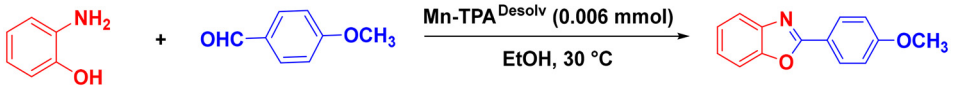

Entry	Solvent	Conversion (%)
1	CH_2Cl_2	56
2	$CHCl_3$	59
3	CH_3CN	72
4	THF	74
5	H_2O	53
6	EtOH	99.9

Reaction conditions: *p*-tolualdehyde (1.1 mmol), *o*-aminophenol (1.0 mmol), catalyst (0.006 mmol), time 10 min, and temperature 30 °C.

in dichloromethane and chloroform with 56% and 59% conversions, respectively (entries 1 and 2, Table 1). In contrast, solvents like acetonitrile and tetrahydrofuran provided 72% and 74% conversions, respectively (entries 3 and 4, Table 1). Polar and protic solvents, water and ethanol, provided 53% and 99.9% conversions, respectively (entries 5 and 6, Table 1). Screening of solvents suggested ethanol as the most effective solvent among those tested, providing good to excellent results in the synthesis of benzoxazole derivatives. Ethanol is effective in this reaction for several reasons. As a polar protic solvent, ethanol can form hydrogen bonds with *o*-amino phenol, helping to stabilize the reactants and enhance their interaction in the reaction medium. This solvent improves the solubility of the substrates, ensuring efficient diffusion of the reactants into the manganese active sites of the **Mn-TPA^{Desolv}** MOF and forming benzoxazole products in high conversions. Furthermore, the environment friendly and non-toxic nature of ethanol also makes it ideal for green chemistry applications. Consequently, ethanol was selected as the optimized solvent for subsequent catalytic reactions.

After optimization of the reaction conditions, to assess generality and the broad substrate scope, several aryl aldehydes containing electron-withdrawing and electron-donating groups were examined under optimized conditions. The optimized reaction conditions were found to produce good conversion regardless of whether the aryl aldehydes exhibited electron-withdrawing or electron-donating groups. On a gram scale synthesis, experiments were performed where aldehydes (55 mmol) reacted with *o*-aminophenol (50 mmol) in ethanol at 30 °C in the presence of the **Mn-TPA^{Desolv}** catalyst (Fig. 3). Benzaldehyde demonstrated excellent catalytic performance and achieved 99.9% conversion of benzoxazole within 30 min, accompanied by a high TON of 8325 and TOF of 277 min^{-1} (entry 1, Fig. 3). The aryl aldehydes bearing electron-withdrawing groups like –F, –Cl, –Br, $–NO_2$, and –CN afforded excellent 98–99.9% conversion of the desired products of benzoxazole derivatives, within 45 min accompanied by a high TON of 8166–8325 and TOF of 181–185 min^{-1} (entries 2–6, Fig. 3). The aryl aldehydes bearing electron-donating groups like *m*-methoxybenzaldehyde, *p*-methoxybenzaldehyde, and *p*-tolualdehyde resulted in 99.9% conversion of the desired products within 60 min accompanied by a high TON of 8325 and TOF of 138 min^{-1} (entries 7–9, Fig. 3). To check if the reaction occurs on the surface or within the pores, a sterically hindered bulky substrate, 1-naphthaldehyde, was used in the reaction. It is obvious that if the reaction occurs on the surface, increasing the size of the substrates is unlikely to significantly affect the conversion. Conversely, if the reaction occurs within the pores, an increase in the size of the reactants could hinder their diffusion into the inner cavities and it will significantly impact the conversion.

Interestingly, 1-naphthaldehyde was observed to effectively produce the corresponding product with excellent 99.9% conversion within 90 min accompanied by a high TON of 8325 and TOF of 92 min^{-1} (entry 10, Fig. 3). The result of the bulky substrate indicates that increasing the size of the aldehyde substrate has no effect on percentage conversion. This suggests that the reaction takes place on the surface of **Mn-TPA^{Desolv}** and is also supported by our previous studies on cyanosilylation reactions.[39,40] The percentage conversion of all catalytic reactions was confirmed by ^{1}H NMR spectroscopy (Fig. S9–S18†). The results suggest that aldehydes with electron-withdrawing substituents react faster and have high TOF values, compared to those with electron-donating substituents. In comparison bulkier substrates exhibited slow reaction rates and comparatively low TOF values. This indicates that both electronic effects and steric factors play important roles in determining the reaction rate. Additionally, the **Mn-TPA^{Desolv}** catalyst is highly efficient for benzoxazole derivative synthesis.

The heterogeneity test is one of the crucial control tests in heterogeneous catalysis. For this study, a filtration test was performed using *o*-aminophenol and *p*-tolualdehyde in ethanol at 30 °C under optimized reaction conditions (Fig. 4). After two minutes, the **Mn-TPA^{Desolv}** catalyst was filtered out. The reaction with the filtrate was then allowed to proceed under similar reaction conditions without the solid catalyst for an additional 30 min. Samples were collected periodically and analyzed using ^{1}H NMR spectroscopy. No significant progress was observed in the reaction after the removal of **Mn-TPA^{Desolv}**. This indicates that no active functional species were present inside the reaction mixture, proving the truly heterogeneous nature of the **Mn-TPA^{Desolv}** catalyst.

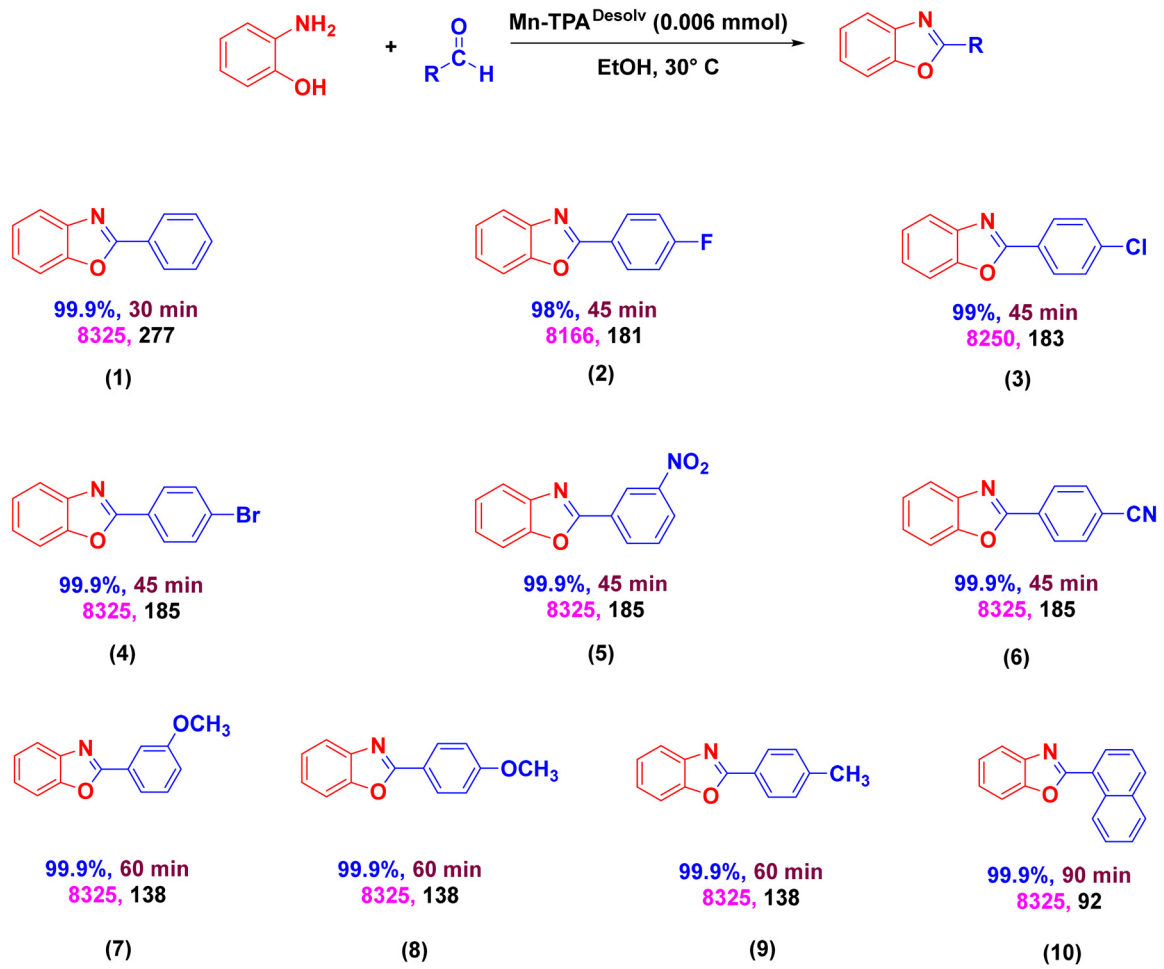

Fig. 3 Results of the synthesis of benzoxazole derivatives using **Mn-TPA^{Desolv}**. Reaction conditions: aldehydes (55 mmol), *o*-aminophenol (50 mmol) and **Mn-TPA^{Desolv}** (0.006 mmol) at 30 °C in ethanol. The blue text indicates percentage conversion, the wine text indicates time, the pink text indicates TON and the black text indicates TOF (min^{-1}).

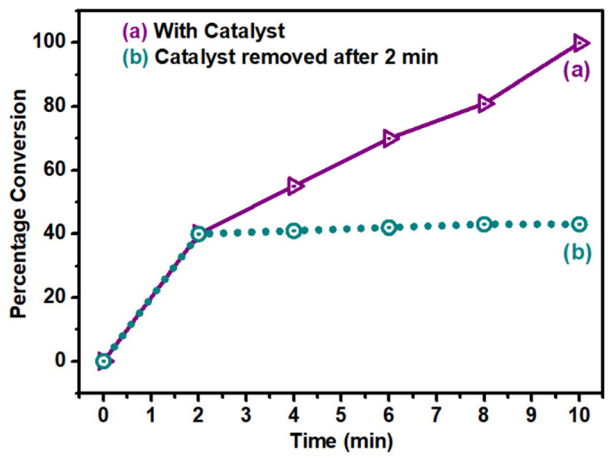

Fig. 4 Heterogeneity study of the **Mn-TPA^{Desolv}** catalyst for the synthesis of benzoxazoles using *p*-tolualdehyde and *o*-aminophenol.

The catalytic activity of **Mn-TPA^{Desolv}** is compared with other reported homogeneous and heterogeneous catalysts for benzoxazole synthesis and the results are summarized in Table S2.† As shown in Table S2,† **Mn-TPA^{Desolv}** exhibits superior catalytic performance under mild and sustainable reaction conditions compared to other previously reported catalysts. Some of the catalysts mentioned in the table (entries 7, 10 and 11, Table S2†) also produce desired products with good conversion; however, they require high-temperature and extended reaction time. Therefore, it can be concluded that **Mn-TPA^{Desolv}** acts as a highly efficient and facile heterogeneous catalyst for the synthesis of benzoxazole derivatives.

Synthesis of benzimidazole derivatives

Inspired by the excellent catalytic performance of **Mn-TPA^{Desolv}** in synthesizing benzoxazole derivatives, this catalyst has also been employed as an effective heterogeneous catalyst for the synthesis of benzimidazole derivatives. To optimize the reaction, *p*-chlorobenzaldehyde (1 mmol) and *o*-phenylenediamine (1 mmol) were chosen as model substrates using ethanol.

Using 0.004 mmol **Mn-TPA^{Desolv}** led to 82% conversion within 10 min (entry 1, Table S3†). Further experiments revealed that increasing the catalyst amount to 0.005 mmol resulted in 69% and 82% conversions within 6 and 8 min, respectively (entries 2 and 3, Table S3†). However, this reaction with 0.005 mmol **Mn-TPA^{Desolv}** catalyst at 30 °C for 10 min achieved an excellent conversion of 99.9% (entry 4, Table S3†). Increasing the catalyst loading to 0.006–0.007 mmol under similar reaction conditions led to 99.9% conversion of benzimidazole derivatives without affecting the reaction time (entries 5 and 6, Table S3†). Further increasing the reaction temperature to 40 °C and 50 °C using 0.005 mmol catalyst reduced the required time to achieve 99.9% conversion in 8 and 6 min, respectively (entries 7 and 8, Table S3†). Therefore, to minimize energy consumption, subsequent catalytic reactions were performed at 30 °C for 10 min. The as-synthesized MOF, **Mn-TPA**, exhibited a significantly lower conversion (49%) compared to the desolvated MOF, **Mn-TPA^{Desolv}** (entry 9, Table S3†). This emphasizes the critical role and efficiency of OMSs in enhancing conversion rates. When the acid ligand (TPA) was used, no conversion was observed while the metal source $Mn(NO_3)_2{\cdot}4H_2O$ provided only trace conversion under optimized conditions (entries 10 and 11, Table S3†). This reaction was also performed without a catalyst, resulting in no desired products (entry 12, Table S3†). Therefore, this reaction showed that the presence of a catalyst is essential to obtain the desired conversion of the product. These results highlight the important role of desolvation in enhancing the catalytic activity, making **Mn-TPA^{Desolv}** the preferred catalyst over the as-synthesized MOF or its individual components. Notably, a loading of 0.005 mmol **Mn-TPA^{Desolv}** was sufficient to facilitate efficient reaction progress with excellent conversion. Thus, a catalyst loading of 0.005 mmol **Mn-TPA^{Desolv}** was chosen for subsequent catalytic reactions.

Effect of solvents towards the synthesis of benzimidazole derivatives

For benzimidazole derivative synthesis, we have tested solvents such as chloroform, ethanol, water, dichloromethane, acetonitrile and tetrahydrofuran. The reaction of *p*-chlorobenzaldehyde and *o*-phenylenediamine in chloroform provided 35% conversion (entry 1, Table 2). In comparison, solvents like dichloromethane, tetrahydrofuran and acetonitrile showed conversions of 43%, 47% and 84%, respectively (entries 2–4, Table 2). Polar and protic solvents such as water and ethanol exhibited significantly higher conversions of 50% and 99.9%, respectively. This screening of the solvent study highlights ethanol as the most efficient solvent, provided excellent percentage conversion for the synthesis of benzimidazole derivatives (entries 5 and 6, Table 2) as well. Therefore, ethanol was chosen for further catalytic reactions.

After optimizing the reaction conditions, various aromatic aldehydes with electron-withdrawing and electron-donating groups were evaluated under optimized conditions to assess the broad substrate scope. The optimized reaction conditions achieved excellent conversion, irrespective of whether the aromatic aldehydes containing electron-withdrawing or electron-donating groups.

On a gram scale synthesis, experiments were conducted in which aldehydes (50 mmol) reacted with *o*-phenylenediamine (50 mmol) in ethanol at 30 °C in the presence of **Mn-TPA^{Desolv}** (Fig. 5). Benzaldehyde exhibited remarkable 99.9% conversion of the desired product within 30 min, along with an impressive high TON of 9990 and TOF of 333 min^{-1} (entry 1, Fig. 5). The aromatic aldehydes containing electron-withdrawing groups such as –F, –Cl, $–NO_2$ and –CN exhibited an excellent 99.9% conversion of the desired products within 30 min, along with an impressive high TON of 9990 and TOF of 333 min^{-1} (entries 2–7, Fig. 5) While *p*-bromobenzaldehyde exhibited 99.9% conversion within 45 min accompanied by a high TON of 9990 and TOF of 222 min^{-1} (entry 8, Fig. 5). The aromatic aldehydes containing electron-donating groups like *p*-tolualdehyde, *o*-tolualdehyde, and *p*-methoxybenzaldehyde resulted in 99.9% conversion of the desired products within 45 min accompanied by a high TON of 9990 and a TOF of 222 min^{-1} (entries 9–11, Fig. 5). To assess whether the reaction occurs on the surface or inside the pores, bulky substrates such as 1-naphthaldehyde and 9-anthracenecarboxaldehyde were used in the reaction. Interestingly, both the sterically hindered

Table 2 Synthesis of benzimidazole using *p*-chlorobenzaldehyde and **Mn-TPA^{Desolv}** in different solvents

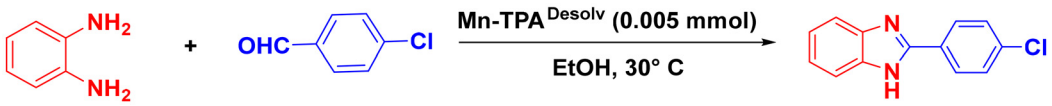

Entry	Solvent	Conversion (%)
1	$CHCl_3$	35
2	CH_2Cl_2	43
3	THF	47
4	MeCN	84
5	H_2O	50
6	EtOH	99.9

Reaction conditions: *p*-chlorobenzaldehyde (1.0 mmol), *o*-phenylenediamine (1.0 mmol), catalyst (0.005 mmol), time 10 min, and temperature 30 °C.

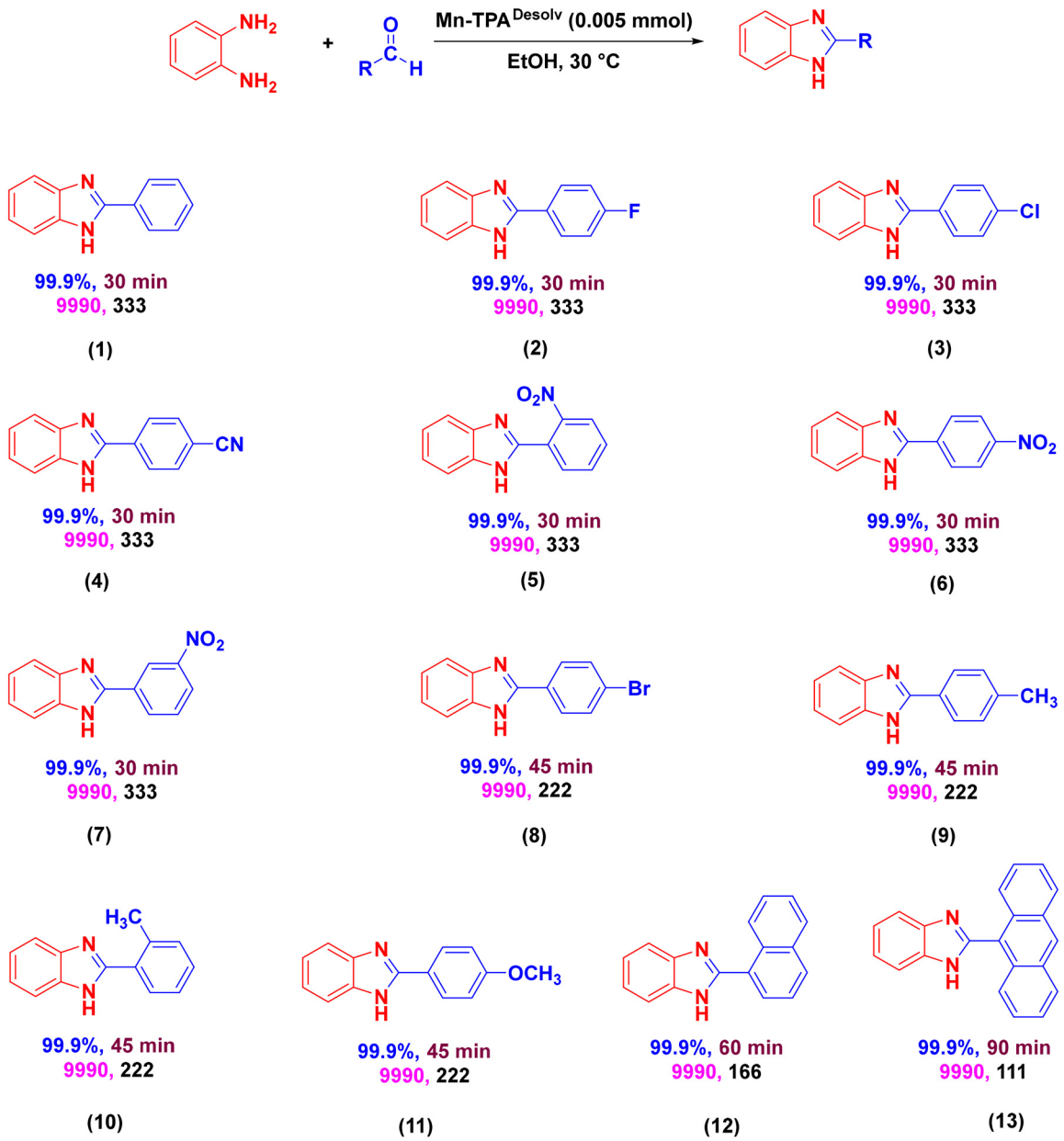

Fig. 5 Results of the synthesis of benzimidazole derivatives using the **Mn-TPA^{Desolv}** catalyst. Reaction conditions: aldehyde (50 mmol), *o*-phenylenediamine (50 mmol) and **Mn-TPA^{Desolv}** (0.005 mmol) at 30 °C. The blue text indicates percentage conversion, the wine text indicates time, the pink text indicates TON and the black text indicates TOF (min^{-1}).

bulky substrates 1-naphthaldehyde and 9-anthracenecarboxaldehyde exhibit an excellent conversion, a high TON and a high TOF towards the conversion of corresponding benzimidazole derivatives. The substrate 1-naphthaldehyde demonstrated 99.9% conversion of the desired product within 60 min achieving a high TON of 9990 and TOF of 166 min^{-1} (entry 12, Fig. 5). Whereas 9-anthracenecarboxaldehyde provided 99.9% conversion with a prolonged reaction time (90 min) accompanied by a high TON of 9990 and TOF of 111 min^{-1} (entry 13, Fig. 5). The results from bulky substrates show that increasing the size of the aldehyde substrates did not affect the reaction conversion, indicating that the reaction occurs on the surface of **Mn-TPA^{Desolv}**. The percentage conversion of all the products was confirmed through ^{1}H NMR spectroscopy (Fig. S19–S31†). The results indicate that aldehydes bearing electron-withdrawing groups react faster and have higher TOF values compared to those with electron-donating groups. In contrast, bulkier substrates show slower reaction rates and lower TOF values. It highlights the influence of both electronic and steric effects on the reaction rate. Furthermore, **Mn-TPA^{Desolv}** exhibits high efficiency in the synthesis of benzimidazole derivatives.

To check the heterogeneity of the **Mn-TPA^{Desolv}** catalyst, a filtration experiment was conducted using *p*-chlorobenzaldehyde and *o*-phenylenediamine at 30 °C in ethanol (Fig. 6). The **Mn-TPA^{Desolv}** catalyst was removed by filtration after two minutes of reaction. The resulting filtrate without a catalyst was allowed to react further under similar reaction conditions. At regular intervals, the samples were collected and analyzed using ^{1}H NMR spectroscopy. There was no noticeable progress in percentage conversion after removal of the **Mn-TPA^{Desolv}** catalyst. This suggests that no homogeneous species was present in the reaction mixture. This confirms the truly heterogeneous nature of the **Mn-TPA^{Desolv}** catalyst.

It is widely recognized that the recyclability of a heterogeneous catalyst is a critical factor for its commercialization and large-scale industrial implementation. In this context, the reusability of **Mn-TPA^{Desolv}** was examined in the reaction involving *p*-chlorobenzaldehyde and *o*-phenylenediamine (Fig. 7). After completion of the catalytic reaction, **Mn-TPA^{Desolv}** was recovered by centrifugation of the reaction mixture, followed by filtration and washing with acetone. The catalyst was dried for 5 h and activated under a high vacuum pump overnight at 120 °C. It was then reused 30 times for recyclability testing. The filtered solution was analyzed using ^{1}H NMR spectroscopy after each cycle. As illustrated in Fig. 7, 99.9% conversion was obtained in each cycle, demonstrating the remarkable efficiency of the **Mn-TPA^{Desolv}** catalyst.

In order to evaluate the stability of the catalyst during the 30 cycles of catalysis, PXRD patterns were recorded after each cycle. Fig. 8 shows that PXRD pattern of each catalytic reactions are similar to the PXRD pattern of the activated MOF (**Mn-TPA^{Desolv}**). This suggests that the structural integrity of the MOF catalyst was intact for 30 cycles, confirming the robust nature of **Mn-TPA^{Desolv}**.

Furthermore, the catalytic performance of **Mn-TPA^{Desolv}** is evaluated in comparison with various reported homogeneous and heterogeneous catalysts for the synthesis of benzimidazoles (Table S4†). Notably, the **Mn-TPA^{Desolv}** catalyst demonstrates excellent catalytic performance under mild conditions surpassing the performance of many previously reported catalysts. Several catalysts mentioned in the table (entries 6, 9, 10 and 12, Table S4†) produced desired product formation with significant conversion, although required elevated temperature and prolonged reaction time. In contrast, the results demonstrate that **Mn-TPA^{Desolv}** is a highly efficient heterogeneous catalyst for the synthesis of benzimidazole derivatives.

Following the literature, a plausible mechanism for the synthesis of benzoxazoles and benzimidazoles from *o*-aminophenol or *o*-phenylenediamine with aromatic aldehydes is depicted in Fig. 9.[1,4,6,7] Initially, the aldehyde molecule is activated by the Lewis acid site of manganese present on the **Mn-TPA^{Desolv}** catalyst *via* Mn···O coordinative interaction (see Fig. 9). The electrophilicity of the carbonyl carbon on the acti-

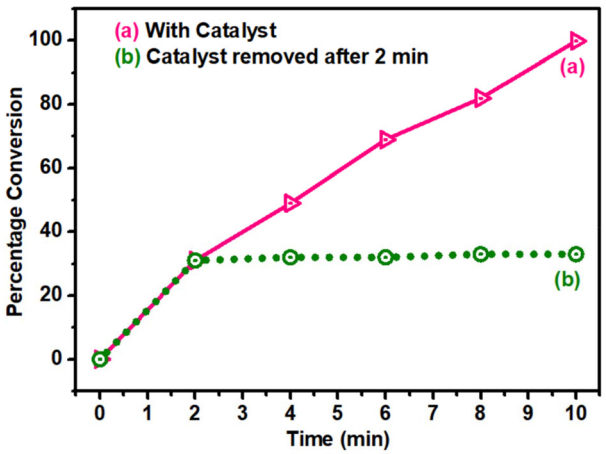

Fig. 6 Percentage conversion *vs.* time graph for the synthesis of benzimidazole derivatives using *p*-chlorobenzaldehyde with **Mn-TPA^{Desolv}** as a catalyst.

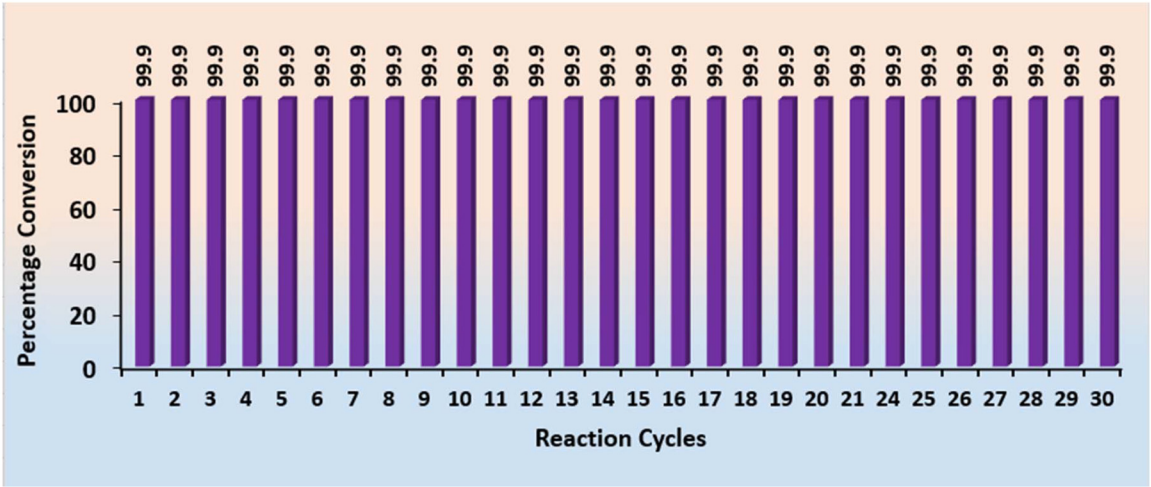

Fig. 7 Recyclability results of **Mn-TPA^{Desolv}** in the synthesis of benzimidazole derivatives using *p*-chlorobenzaldehyde for 30 consecutive catalytic cycles.

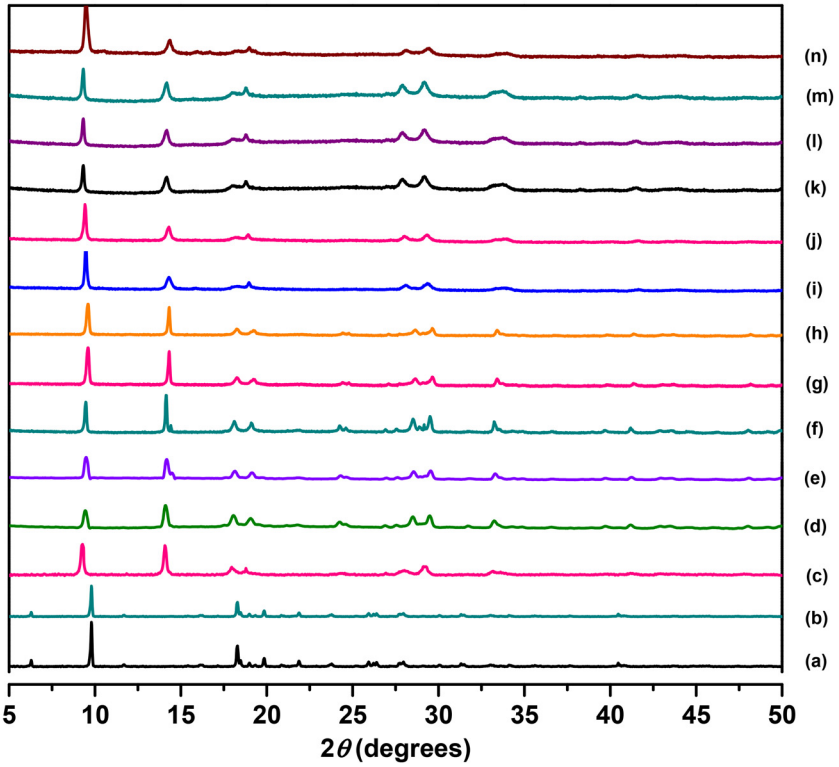

Fig. 8 PXRD patterns of the recyclability of **Mn-TPA** MOF at various stages: (a) simulated; (b) as-synthesized; (c) **Mn-TPA^{Desolv}**; (d) after the 1st catalytic cycle; (e) after the 3rd catalytic cycle; (f) after the 6th catalytic cycle; (g) after the 9th catalytic cycle; and (h) after the 12th catalytic cycle; (i) after the 15th catalytic cycle; (j) after the 18th catalytic cycle; (k) after the 21st catalytic cycle; (l) after the 24th catalytic cycle; (m) after the 27th catalytic cycle; and (n) after the 30th catalytic cycle.

vated aldehyde increases, facilitating the attack of the amino group of *o*-aminophenol or *o*-phenylenediamine on carbonyl carbon. Due to proton transfer and subsequent elimination of a water molecule as a byproduct, a stable imine (C═N) bond is formed. Furthermore, a ring closure reaction occurs through intramolecular nucleophilic attack of an *ortho*-substituted OH or amine group (–XH, X = O or NH) with the carbon atom of the imine group. Subsequently, proton transfer occurs, followed by a dehydrogenation process facilitated by oxidative aromatization. Finally, a stable desired product is successfully formed followed by the recovery of the **Mn-TPA^{Desolv}** catalyst. The regenerated catalyst reactivates as an effective active site to facilitate the formation of the desired product in subsequent reaction cycles.

Experimental methods

Materials

All the reagents and solvents were supplied by Merck and Central Drug House chemical companies and used without any further purification.

Physical measurements

Powder X-ray diffraction (PXRD) patterns were recorded using a Rigaku Miniflex 600 using Cu-Kα radiation (λ = 1.54 Å) in the 2θ range of 5–50°. Fourier transform infrared (FT-IR) spectra were recorded using a Bruker Alpha machine in the region of 4000–600 cm^{-1}. Thermogravimetric analysis (TGA) data were acquired using a Shimadzu DTG-60H instrument from 50 to 600 °C at a heating rate of 10 °C min^{-1} under a N_2 gas flow. ^{1}H NMR spectra were recorded using a Bruker 400 MHz spectrometer and a Magritek model Spinsolve spectrometer at a frequency of 80 MHz, using $CDCl_3$ and DMSO-d_6 solvents and tetramethylsilane as an internal reference. The acidic and basic properties were determined by temperature-programmed desorption of ammonia (NH_3-TPD) using a BELCAT II instrument. Morphological studies have been performed using a Zeiss Gemini SEM 500 field emission scanning electron microscope (FE-SEM). X-ray Photoelectron Spectroscopy (XPS) measurements were performed using a Thermo Fisher instrument, equipped with Al-Kα radiation as the excitation source.

Preparation

Preparation of Mn-TPA. The **Mn-TPA** MOF was prepared *via* a solvothermal method based on procedures outlined in ref. 39, 40 and 49. Initially, a Teflon-lined stainless steel autoclave was loaded with 1.0 mmol $Mn(NO_3)_2{\cdot}4H_2O$, 1.0 mmol terephthalic acid and 10 mL of DMF. The obtained solution was stirred for 30 min and then the vessel was closed and placed in an oven that was previously kept at 120 °C. The reaction was

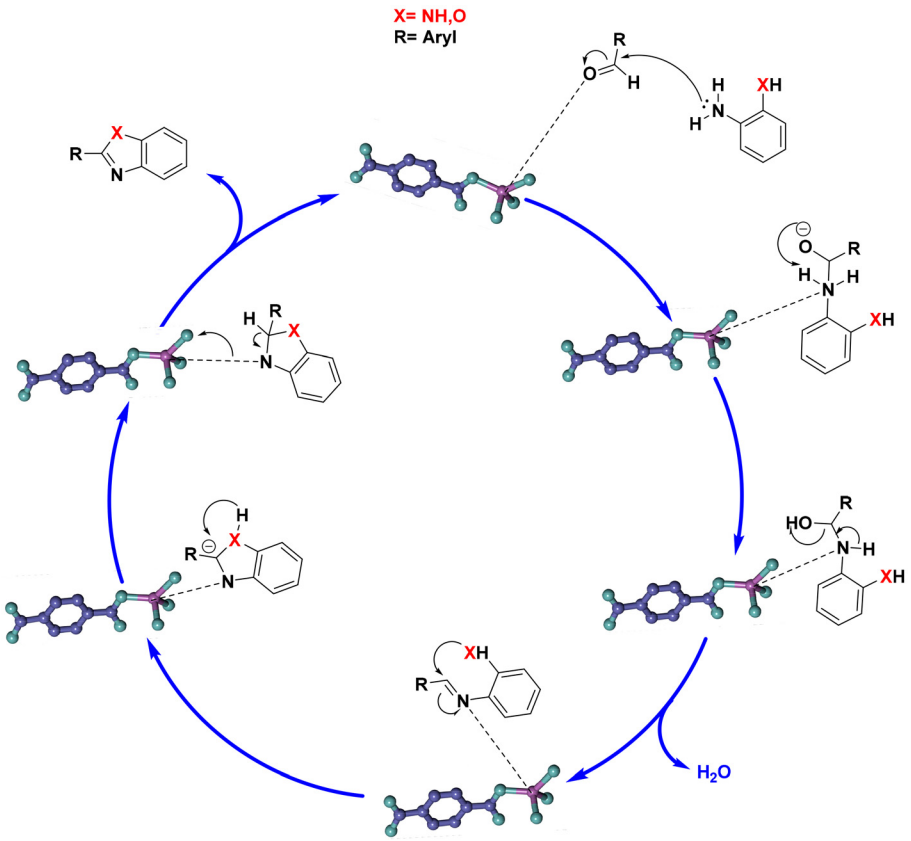

Fig. 9 Proposed mechanism for the synthesis of benzoxazole and benzimidazole derivatives with the **Mn-TPA^{Desolv}** catalyst.

continued for 48 hours. After cooling the autoclave to room temperature, transparent crystals were formed. The reaction mixture was filtered and washed with DMF several times and dried under vacuum in a desiccator. The **Mn-TPA** transparent crystals were obtained with an 85% yield based on manganese. Anal. calcd for $C_{22}H_{22}N_2Mn_2O_8$: C, 45.35; H, 3.76; N, 4.80. Found: C, 44.56, H, 4.05; N, 4.60. IR: νas(OCO), 1538; νs(OCO), 1374 (Fig. S1†).

Preparation of Mn-TPA^{Desolv}. The **Mn-TPA** MOF was subjected to heating at 120 °C for 12 h under high vacuum to ensure the complete removal of coordinated DMF molecules and moisture, allowing the manganese sites to become accessible to substrate molecules. Anal. calcd for $C_{16}H_8Mn_2O_8$: C, 43.84; H, 1.87. Found: C, 43.54; H, 2.08. The lack of N indicates that the DMF solvent has been entirely removed upon heating at 120 °C. IR: νas(OCO), 1555; νs(OCO), 1383 (Fig. S2†).

Catalytic experiments

Procedure for the synthesis of benzoxazole derivatives using the Mn-TPA^{Desolv} catalyst. A round bottom flask was loaded with *o*-aminophenol (1.0 mmol), aldehyde (1.1 mmol) and 0.006 mmol **Mn-TPA^{Desolv}** catalyst in ethanol at 30 °C, followed by stirring the reaction mixture for 10 min. Upon completion of the reaction, monitored by TLC and ^{1}H NMR spectroscopy, the catalyst was separated by filtration, and the organic solvent was evaporated to obtain the concentrated product. The collected product was dissolved in $CDCl_3$ and examined *via* ^{1}H NMR spectroscopy to determine the percentage conversion of the product.

Procedure for the synthesis of benzimidazole derivatives using the Mn-TPA^{Desolv} catalyst. A round bottom flask was loaded with a mixture of *o*-phenylenediamine (1.0 mmol), aldehyde (1.0 mmol) and 0.005 mmol **Mn-TPA^{Desolv}** catalyst in ethanol at 30 °C, followed by stirring the reaction mixture for 10 min. Upon completion of the reaction, monitored by TLC and ^{1}H NMR spectroscopy, the catalyst was separated by filtration, and the organic solvent was evaporated to obtain the concentrated product. The collected product was dissolved in $CDCl_3$ and DMSO-d_6, and then examined *via* ^{1}H NMR spectroscopy to determine the percentage conversion of the product.

Bulk-scale procedure for benzoxazole derivatives. A similar procedure to that mentioned above for the synthesis of benzoxazoles was followed with variations in the concentration of substrates. A 100 mL round bottom flask was loaded with *o*-aminophenol (50 mmol), aldehyde (55 mmol), **Mn-TPA^{Desolv}** (0.006 mmol) and 10–15 mL of EtOH, followed by stirring the mixture at 30 °C.

Bulk-scale procedure for benzimidazole derivatives. A similar procedure to that described above was employed for the synthesis of benzoxazoles, by varying the concentration of substrates. A 100 mL round bottom flask was loaded with

o-phenylenediamine (50 mmol), aldehyde (50 mmol), **Mn-TPA^{Desolv}** (0.005 mmol) and 10–15 mL of EtOH, followed by stirring the mixture at 30 °C.

Conclusion

In summary, we demonstrate the exceptional catalytic performance of a robust 3D manganese-based MOF, $\{Mn_2(TPA)_2(DMF)_2\}_n$, where the desolvated form **Mn-TPA^{Desolv}** acts as a highly efficient heterogeneous catalyst due to its accessible manganese open metal sites (OMSs). This material exhibits remarkable activity in synthesizing benzoxazole and benzimidazole derivatives under exceptionally mild conditions (30 °C in ethanol), achieving quantitative conversions (99.9%) across a wide range of aldehydes. Furthermore, the catalyst provides outstanding turnover numbers (TONs up to 9990) and frequencies (TOFs up to 333 min^{-1}) even with challenging sterically hindered substrates like 1-naphthaldehyde and 9-anthracenecarboxaldehyde. The catalyst maintains its structural integrity and highest catalytic efficiency through an unprecedented 30 reaction cycles, demonstrating exceptional stability not commonly observed in MOF-based systems. These combined attributes, including the mild reaction conditions, broad substrate scope, extraordinary TON/TOF values, and exceptional recyclability, not only distinguish **Mn-TPA^{Desolv}** from other reported catalysts but also highlight its strong potential for industrial-scale applications. Furthermore, the versatility of this robust catalytic system suggests promising opportunities for extending its utility to other organic transformations, while structural modifications could further enhance its activity and selectivity for specific applications.

Data availability

The data supporting this article have been included as part of the ESI.†

Conflicts of interest

There are no conflicts to declare.

Acknowledgements

A. C. acknowledges the Department of Science and Technology (DST), New Delhi, India, for a very supportive INSPIRE Faculty Fellowship (DST/INSPIRE/04/2020/001603). P. K. and A. C. gratefully acknowledge research facilities at Jawaharlal Nehru University, New Delhi, and the Central University of Haryana, Mahendergarh. S. K. and Chhaya thank the CSIR, New Delhi, for a senior research fellowship and junior research fellowship, respectively. The authors gratefully acknowledge Soumya Kumar Mondal and Prof. Tapas Kumar Maji, JNCASR, Bangalore, for helping in measurements.

References

1 T. T. Nguyen, X.-T. T. Nguyen, T.-L. H. Nguyen and P. H. Tran, *ACS Omega*, 2019, **4**, 368.
2 A. Kumar, R. A. Maurya and D. Saxena, *Mol. Diversity*, 2009, **14**, 331.
3 A. Chakraborty, S. Bhattacharyya, A. Hazra, A. C. Ghosh and T. K. Maji, *Chem. Commun.*, 2016, **52**, 2831.
4 V. Sankar, P. Karthik, B. Neppolian and B. Sivakumar, *New J. Chem.*, 2020, **44**, 1021.
5 A. Khazaei, A. A. Manesh, H. Ahmadian and H. Veisi, *Appl. Organomet. Chem.*, 2016, **30**, 109.
6 S. Kusuma, D. B. Bawiskar, C. Singh, P. Panneerselvam, P. Sinha, A. K. Samal and A. H. Jadhav, *RSC Adv.*, 2023, **13**, 32110.
7 E. Niknam, F. Panahi, F. Daneshgar, F. Bahrami and A. Khalafi-Nezhad, *ACS Omega*, 2018, **3**, 17135.
8 J. Azizian, P. Torabi and J. Noei, *Tetrahedron Lett.*, 2016, **57**, 185.
9 S. K. Guchhait, G. Priyadarshani and N. M. Gulghane, *RSC Adv.*, 2016, **6**, 56056.
10 H. Xiangming, M. Huiqiang and W. Yulu, *ARKIVOC*, 2007, **13**, 150.
11 M. A. Chari, P. Sadanandam, D. Shobha and K. Mukkanti, *J. Heterocycl. Chem.*, 2010, **47**, 153.
12 Y. Kim, M. R. Kumar, N. Park, Y. Heo and S. Lee, *J. Org. Chem.*, 2011, **76**, 9577.
13 P. L. Reddy, R. Arundhathi, M. Tripathi and D. S. Rawat, *RSC Adv.*, 2016, **6**, 53596.
14 A. Maleki, N. Ghamari and M. Kamalzare, *RSC Adv.*, 2014, **4**, 9416.
15 L. Fan, L. Kong and W. Chen, *Heterocycles*, 2015, **91**, 2306.
16 K. Bahrami, M. M. Khodaei and I. Kavianinia, *J. Chem. Res.*, 2006, **2006**, 783.
17 Y. Venkateswarlu, S. R. Kumar and P. Leelavathi, *Org. Med. Chem. Lett.*, 2013, **3**, 7.
18 S. Lin and L. H. Yang, *Tetrahedron Lett.*, 2005, **46**, 4315.
19 R. S. Harapanhalli, L. W. McLaughlin, R. W. Howell, D. V. Rao, S. J. Adelstein and A. I. Kassis, *J. Med. Chem.*, 1996, **39**, 4804.
20 E. Verner, B. A. Katz, J. R. Spencer, D. Allen, J. Hataye, W. Hruzewicz, H. C. Hui, A. Kolesnikov, Y. Li, C. Luong, A. Martelli, K. Radika, R. Rai, M. She, W. Shrader, P. A. Sprengeler, S. Trapp, J. Wang, W. B. Young and R. L. Mackman, *J. Med. Chem.*, 2001, **44**, 2753.
21 J. J. V. Eynde, F. Delfosse, P. Lor and Y. V. Haverbeke, *Tetrahedron*, 1995, **51**, 5813.
22 I. Bhatnagar and M. V. George, *Tetrahedron*, 1968, **24**, 1293.
23 V. Ravi, E. Ramu, K. Vijay and A. S. Rao, *Chem. Pharm. Bull.*, 2007, **55**, 1254.
24 K. Bahrami, M. M. Khodaei and F. Naali, *J. Org. Chem.*, 2008, **73**, 6835.
25 G. N. Vazquez, H. M. Diaz, F. A. Crespo, I. L. Rivera, R. V. Molina, O. M. Muniz and S. E. Soto, *Bioorg. Med. Chem. Lett.*, 2006, **16**, 4169.
26 M. P. Singh, S. Sasmal, W. Lu and M. N. Chatterjee, *Synthesis*, 2000, 1380.

27 V. R. Ruiz, A. Corma and M. J. Sabater, *Tetrahedron*, 2010, **66**, 730.
28 H. Sharghi, M. Aberi and M. M. Doroodmand, *Adv. Synth. Catal.*, 2008, **350**, 2380.
29 L. Tang, X. Guo, Y. Yang, Z. Zha and Z. Wang, *Chem. Commun.*, 2014, **50**, 6145.
30 G. Brahmachari, S. Laskar and P. Barik, *RSC Adv.*, 2013, **3**, 14245.
31 L.-X. Yun, C. Zhang, X.-R. Shi, Y.-J. Dong, H.-T. Zhang, Z.-G. Shen and J.-X. Wang, *Nanoscale*, 2024, **16**, 691.
32 W. Begum, M. Chauhan, R. Kalita, P. Gupta, N. Akhtar, N. Antil, R. Newar and K. Manna, *ACS Catal.*, 2024, **14**, 10427.
33 S. Basappa, A. Prakash, S. S. Talekar, M. V. Mane and S. K. Bose, *ACS Catal.*, 2024, **14**, 4301.
34 G. Cai, P. Yan, L. Zhang, H.-C. Zhou and H.-L. Jiang, *Chem. Rev.*, 2021, **121**, 12278.
35 A. Bavykina, N. Kolobov, I. S. Khan, J. A. Bau, A. Ramirez and J. Gascon, *Chem. Rev.*, 2020, **120**, 8468.
36 X. Zhang, Z. Chen, X. Liu, S. L. Hanna, X. Wang, R. Taheri-Ledari, A. Maleki, P. Li and O. K. Farha, *Chem. Soc. Rev.*, 2020, **49**, 7406.
37 K. O. Kirlikovali, S. L. Hanna, F. A. Son and O. K. Farha, *ACS Nanosci. Au*, 2023, **3**, 37.
38 P. Yadav, S. Kumari, A. Yadav, P. Bhardwaj, M. Maruthi, A. Chakraborty and P. Kanoo, *ACS Omega*, 2023, **8**, 28367.
39 O. Prakash, D. Verma and P. C. Singh, *J. Mater. Chem. B*, 2024, **12**, 10198.
40 F. Liang, J. Liang, D. Gao, L. Kong, S. Huang, Y. Guo, C. Liu and T. Ding, *CrystEngComm*, 2024, **26**, 1032.
41 X. Zhang, J. Maddock, T. M. Nenoff, M. A. Denecke, S. Yang and M. Schröder, *Chem. Soc. Rev.*, 2022, **51**, 3243.
42 B. Mohanty, S. Kumari, P. Yadav, P. Kanoo and A. Chakraborty, *Coord. Chem. Rev.*, 2024, **519**, 216102.
43 N. Liu, J. Zheng, T. Liu, H. Yan, M. Ji, G.-N. Liu, Y. Li, J. Dou, F. Yang and S. Wang, *Inorg. Chem.*, 2024, **63**, 19117.
44 S. Natarajan and K. Manna, *ACS Org. Inorg. Au*, 2024, **4**, 59.
45 A. Yadav and P. Kanoo, *Chem. – Asian J.*, 2019, **14**, 3531.
46 X.-L. Chang, T. Yan and W.-G. Pan, *Cryst. Growth Des.*, 2024, **24**, 2619.
47 A. Khaleeq, S. R. Tariq and G. A. Chotana, *RSC Adv.*, 2024, **14**, 10736.
48 R. Abazari, S. Sanati, N. Li and J. Qian, *Inorg. Chem.*, 2023, **62**, 18680.
49 M. Sun, R. Abazari, J. Chen, C. M. Hussain, Y. Zhou and A. M. Kirillov, *ACS Appl. Mater. Interfaces*, 2023, **15**, 52581.
50 Y. Pan, S. Sanati, M. Nadafan, R. Abazari, J. Gao and A. M. Kirillov, *Inorg. Chem.*, 2022, **61**, 18873.
51 H. Zhou, G. Zhu, S. Dong, P. Liu, Y. Lu, Z. Zhou, S. Cao, Y. Zhang and H. Pang, *Adv. Mater.*, 2023, **35**, 2211523.
52 T. Lv, G. Zhu, S. Dong, Q. Kong, Y. Peng, S. Jiang, G. Zhang, Z. Yang, S. Yang, X. Dong, H. Pang and Y. Zhang, *Angew. Chem.*, 2023, **135**, e202216089.
53 S. Kumari, A. Yadav, A. Kumari, S. Mahapatra, D. Kumar, J. Sharma, P. Yadav, D. Ghosh, A. Chakraborty and P. Kanoo, *Inorg. Chem.*, 2024, **63**, 7146.
54 A. Yadav, S. Kumari, P. Yadav, A. Hazra, A. Chakraborty and P. Kanoo, *Dalton Trans.*, 2022, **51**, 15496.
55 M. Ren, C. Li, T. Hu, L. Fan and X. Zhang, *Cryst. Growth Des.*, 2024, **24**, 3473.
56 M. Sanz, P. Leo, C. Palomino, M. Paniagua, G. Morales and J. A. Melero, *Green Chem.*, 2024, **26**, 7337.
57 S. Nayab, V. Trouillet, H. Gliemann, P. G. Weidler, I. Azeem, S. R. Tariq, A. S. Goldmann, C. Barner-Kowollik and B. Yameen, *Inorg. Chem.*, 2021, **60**, 4397.
58 K. Rasolinia, H. Arvinnezhad and S. Samadi, *New J. Chem.*, 2025, **49**, 213.
59 Jyoti, S. Kumari, S. Chakraborty, P. Kanoo, V. Kumar and A. Chakraborty, *Dalton Trans.*, 2024, **53**, 15815.
60 W. Fan, K. Liang and J. Liang, *J. Mater. Chem. A*, 2024, **12**, 30318.
61 Y. Geng, H. Tang, Y. Zhang, X. Li, S. Wang, Y. Liu and Y. Gong, *Appl. Organomet. Chem.*, 2025, **39**, e70035.
62 J. Lee, D. Lee, S. Cha, J. Kang, H. Kang, J. Y. Kim and M. Kim, *CrystEngComm*, 2024, **26**, 120.
63 L. H. T. Nguyen, T. T. Nguyen, H. L. Nguyen, T. L. H. Doan and P. H. Tran, *Catal. Sci. Technol.*, 2017, **7**, 4346.
64 R. D. Poulsen, A. Bentien, T. Graber and B. B. Iversen, *Acta Crystallogr., Sect. A: Found. Crystallogr.*, 2004, **60**, 382.
65 S. Gupta, R. Kumar and G. Goel, *Mater. Today Commun.*, 2024, **41**, 110479.
66 W. Zhang, K. Xie, Y. Tang, S. Cheng, M. Qing, Y. Xuan, C. Qin, M. Dong, Y. Zhou and J. Li, *RSC Adv.*, 2022, **12**, 22881.